2018

Quantification of ligand density and stoichiometry on the surface of liposomes using single-molecule fluorescence imaging

Lisa Belfiore
University of Wollongong, lb989@uowmail.edu.au

Lisanne M. Spenkelink
University of Wollongong, lisanne@uow.edu.au

Marie Ranson
University of Wollongong, mranson@uow.edu.au

Antoine M. van Oijen
University of Wollongong, vanoijen@uow.edu.au

Kara L. Vine
University of Wollongong, kara@uow.edu.au

Quantification of ligand density and stoichiometry on the surface of liposomes using single-molecule fluorescence imaging

Abstract

Despite the longstanding existence of liposome technology in drug delivery applications, there have been no ligand-directed liposome formulations approved for clinical use to date. This lack of translation is due to several factors, one of which is the absence of molecular tools for the robust quantification of ligand density on the surface of liposomes. We report here for the first time the quantification of proteins attached to the surface of small unilamellar liposomes using single-molecule fluorescence imaging. Liposomes were surface-functionalized with fluorescently labeled human proteins previously validated to target the cancer cell surface biomarkers plasminogen activator inhibitor-2 (PAI-2) and trastuzumab (TZ, Herceptin®). These protein-conjugated liposomes were visualized using a custom-built wide-field fluorescence microscope with single-molecule sensitivity. By counting the photobleaching steps of the fluorescently labeled proteins, we calculated the number of attached proteins per liposome, which was 11 ± 4 proteins for single-ligand liposomes. Imaging of dual-ligand liposomes revealed stoichiometries of the two attached proteins in accordance with the molar ratios of protein added during preparation. Preparation of PAI-2/TZ dual-ligand liposomes via two different methods revealed that the post-insertion method generated liposomes with a more equal representation of the two differently sized proteins, demonstrating the ability of this preparation method to enable better control of liposome protein densities. We conclude that the single-molecule imaging method presented here is an accurate and reliable quantification tool for determining ligand density and stoichiometry on the surface of liposomes. This method has the potential to allow for comprehensive characterization of novel ligand-directed liposomes that should facilitate the translation of these nanotherapies through to the clinic.

Disciplines

Medicine and Health Sciences

Publication Details

Belfiore, L., Spenkelink, L. M., Ranson, M., van Oijen, A. M. & Vine, K. L. (2018). Quantification of ligand density and stoichiometry on the surface of liposomes using single-molecule fluorescence imaging. Journal of Controlled Release, 278 80-86.

Quantification of ligand density and stoichiometry on the surface of liposomes using single-molecule fluorescence imaging

Lisa Belfiore[a, #], Lisanne M. Spenkelink[b,c, #], Marie Ranson[a], Antoine M. van Oijen[b], Kara L. Vine[a *]

[a]School of Biological Sciences, Centre for Medical and Molecular Bioscience, Illawarra Health and Medical Research Institute, University of Wollongong, New South Wales, Australia

[b]School of Chemistry, Centre for Medical and Molecular Bioscience, Illawarra Health and Medical Research Institute, University of Wollongong, New South Wales, Australia

[c]Zernike Institute for Advanced Materials, University of Groningen, Groningen, The Netherlands

[#] Both authors have contributed equally to this work

*Corresponding author

Correspondence should be addressed to:

Dr Kara L. Vine

Targeted Cancer Therapeutics Laboratory

Illawarra Health and Medical Research Institute

University of Wollongong

Northfields Avenue Wollongong NSW 2522 Australia

Email: kara@uow.edu.au

Telephone: +61 2 4221 4256

Abstract

Despite the longstanding existence of liposome technology in drug delivery applications, there have been no ligand-directed liposome formulations approved for clinical use to date. This lack of translation is due to several factors, one of which is the absence of molecular tools available for the robust quantification of ligand density on the surface of liposomes. We report here for the first time the quantification of proteins attached to the surface of small unilamellar liposomes using single-molecule fluorescence imaging. Liposomes were surface-functionalized with fluorescently-labeled human proteins previously validated to target cancer cell surface biomarkers: plasminogen activator inhibitor-2 (PAI-2) and trastuzumab (TZ, Herceptin®). These protein-conjugated liposomes were then visualized using a custom-built wide-field fluorescence microscope with single-molecule sensitivity. By counting the photobleaching steps of the fluorescently-labeled proteins, we calculated the number of attached proteins per liposome, which was in the range of 1-11 proteins for single-ligand liposomes. Imaging of dual-ligand liposomes revealed stoichiometries of the two attached proteins in accordance with the molar ratios of protein added during preparation. Preparation of PAI-2/TZ dual-ligand liposomes via two different methods revealed that the post-insertion method generated liposomes with a more equal representation of the two differently-sized proteins, demonstrating the ability of this preparation method to control protein densities. We conclude that the single-molecule imaging method presented here is an accurate and reliable quantification tool for determining ligand stoichiometry on the surface of liposomes. This method has the potential to allow for comprehensive characterization of novel ligand-directed liposomes that should facilitate the translation of these nanotherapies through to the clinic.

Keywords: functionalized liposomes, ligand quantification, single-molecule fluorescence microscopy, molecular characterization

1. Introduction

Liposomes have been utilized as delivery systems for drugs and other molecules *in vivo* for several decades [1]. In the context of cancer therapy, liposome-based drug formulations have demonstrated distinct advantages over free drug, including the improved solubility of encapsulated drugs, increased *in vivo* circulation time, reduction in systemic toxicity of the drug and increased delivery to the tumor site [2]. The superior activity of drug-loaded liposomes relies on a multi-step process involving both passive and active targeting mechanisms. Passive targeting is primarily mediated by the enhanced permeability and retention effect [3]. This phenomenon is characterized by the extravasation and retention of small particles into the tumor interstitial space due to highly porous tumor vasculature and poor lymphatic drainage from the tumor site [4]. The prolonged retention of liposomes in the vicinity of the tumor increases the local drug concentration, either when drug released from the liposomes is taken up by tumor cells, or when liposomes containing the drug are internalized by tumor cells [5]. Passive targeting, therefore, reduces off-target effects by preferentially accumulating drug-loaded liposomes in the vicinity of the tumor while reducing the exposure of normal cells to the cytotoxic drug.

Active targeting is achieved via conjugation of one or more ligands to the liposome surface, with that ligand binding to a target receptor(s) expressed on the tumor cell surface [6]. Following liposome extravasation into the tumor interstitial space, subsequent ligand-directed surface binding and internalization (usually via receptor-mediated endocytosis) promotes liposome and drug entry into specific cell types [7]. As actively targeted liposome formulations combine both passive and active drug-delivery mechanisms, actively targeted liposomes can show superior drug delivery to non-targeted liposomes [8]. Liposomes with one or more targeting moieties that facilitate active uptake into cells are termed ligand-directed liposomes. In the context of cancer therapy, the development of dual-ligand-directed

liposomes that can actively target more than one tumor cell subtype and/or stromal cell populations may help overcome therapeutic limitations caused by the intratumoral heterogeneity of cancer [9, 10].

Despite extensive research and development of nanoparticle-based therapeutics, all clinically approved liposome formulations are non-ligand-directed, with efficacies relying solely on passive targeting and accumulation [11]. A comprehensive list can be found elsewhere [12]. Active targeting strategies using liposomes have been extensively explored in the preclinical setting, particularly liposomes targeting tumor-associated receptors, with many reported formulations demonstrating improved efficacy over non-ligand-directed liposomes [13, 14]. Given the general movement in the field towards actively targeted nanotherapeutics, the lack of translation of ligand-directed liposome formulations into clinical practice is somewhat surprising [15]. Previous reviews have identified some of the likely reasons for this phenomenon, ranging from methodological difficulties involved in the large-scale preparation of ligand-directed liposomes, to the limitations of evaluating their efficacy in preclinical models that fail to adequately recapitulate human tumors [16]. For example, once liposomes are administered intravenously, nonspecific interactions of liposomes with a range of plasma proteins may result in the formation of a protein 'corona' at the liposome surface, effectively shielding liposome-bound targeting ligands from interacting with their target receptors and therefore negating their intended tumor cell targeting effect [17].

The absence of molecular tools for the robust characterization of complex liposomes may also be contributing to the lack of clinically approved ligand-directed liposomes. Specifically, no methodology exists to quantify the number of ligands covalently bound to the surface of liposomes. Estimation of ligand conjugation is possible based on preparation parameters, but direct measurement of total surface-bound protein using standard biochemical assays have their limitations. For example, measurement of surface-bound

protein in an actively targeted liposome formulation using colorimetric biochemical methods is challenging due to phospholipid interference in the measurement of very low protein concentrations [18]. While such measurements could potentially quantify the total protein in a sample, they cannot provide information about the number of ligands per liposome in a formulation. Flow cytometric methods that detect the insertion of fluorescently labeled micelles into liposomes as a proxy for successful liposome functionalization have been reported, but are indirect and semi-quantitative [19]. The lack of quantitative methodology poses a particular challenge for the development of liposomes with more than one surface-bound ligand, since the determination of ligand stoichiometry is important for controlling for batch-to-batch variability in the laboratory and for clinical production. The absence of rigorous quantification protocols hinders high-quality large-scale manufacturing of ligand-directed liposome formulations, which may introduce regulatory barriers and slow down their introduction to the clinic.

We describe here the use of single-molecule methods to enable the quantitative characterization of ligand-coupled liposomal drug delivery systems. By removing ensemble averaging, single-molecule approaches allow the direct visualization of population distributions and the precise characterization of sub-populations. These methods have already proven to be important biophysical tools to study a wide variety of biological processes [20-22]. Single-molecule microscopy remains, however, an underutilized technique in therapeutics development. In this study, we report the quantification of protein attachment to the surface of single and dual ligand-directed liposomes using single-molecule fluorescence microscopy. This method allows the detection and quantification of the density of proteins attached to liposomes, facilitating the characterization and translation of ligand-directed liposomes for targeted cancer therapy, and other, applications.

2. Materials and Methods

2.1. Labeling proteins with fluorophores

Human recombinant plasminogen activator inhibitor-2 (PAI-2, SerpinB2), produced in-house by previously published methods [23], and trastuzumab (TZ, Herceptin®; Genentech, CA, USA) were labeled with CF488 or CF647 succinimidyl ester fluorescent dyes (Sigma-Aldrich, MO, USA) as per the manufacturer's instructions. Absorbance at 280 nm (protein) and 488 nm or 647 nm (dye) was used to calculate the protein concentration and degree of labeling (DOL). DOL was further confirmed by electrospray ionization mass spectrometry (ESI-MS).

2.2. Electrospray ionization mass spectrometry (ESI-MS)

Positive ion mass spectra of unlabeled and labeled proteins were acquired on a quadrupole time of flight mass spectrometer (Q-TOF-MS) (Micromass Q-TOF Ultima; Waters, MA, USA) fitted with a Z-spray ionization source. Samples in phosphate-buffered saline (PBS, pH 7.4) were exchanged into deionized water containing 0.1% formic acid and made up to a final concentration of approximately 10 μM. The mass spectra were acquired with a capillary voltage of 2.6 kV, cone voltage of 50 V, source block temperature of 40 °C, and a resolution power of 5000 Hz. Cesium iodide was used for external calibration. Mass was calculated using MassLynx MS V4.1 (Waters, MA, USA).

2.3. Preparation of liposomes

Liposomes were prepared using the thin film hydration method as described previously [24]. Dipalmitoylphosphatidylcholine (DPPC), cholesterol, 1,2-distearoyl-*sn*-glycero-3-phosphoethanolamine-N-[(polyethylene glycol)-2000] (mPEG$_{2000}$-DSPE) and 1,2-distearoyl-*sn*-glycero-3-phosphoethanolamine-N-[maleimide(polyethylene glycol)-2000] (mal-PEG$_{2000}$-DSPE) (Avanti Polar Lipids, AL, USA) in a 20:10:0.8:0.2 molar ratio (conventional method) or DPPC, cholesterol and mPEG$_{2000}$-DSPE in a 20:10:0.6 molar ratio (post-insertion method)

were dissolved in chloroform/methanol (2:1 v/v). For colocalization experiments, liposomes were labeled with Octadecyl Rhodamine B Chloride (R18; Invitrogen, CA, USA) by adding R18 to the chloroform/methanol solution in a 160:1 molar ratio (liposome phospholipid:R18). Organic solvents were removed by rotary evaporation and subsequent freeze drying to form a lipid film. Phospholipids were reconstituted in degassed HEPES buffer (115 mM NaCl, 20 mM HEPES, 2.4 mM K_2PO_4, 1.2 mM $CaCl_2$, 1.2 mM $MgCl_2$; pH 7.4) at a concentration of 20 mM. Once reconstituted, liposomes were passed once through a 0.22 μm PVDF membrane (Merck Millipore, MA, USA) and then serially extruded 11 times through a 0.1 μm PVDF membrane using a syringe-driven extruding apparatus (Avanti Polar Lipids, AL, USA) at a temperature of 50°C (above the phase-transition temperature of DPPC). Liposomes were analyzed by dynamic light scattering to determine particle diameter using a Zetasizer APS (Malvern Instruments, Malvern, UK). Liposomes were surface-functionalized with CF647 labeled PAI-2 and/or CF488 labeled PAI-2 or TZ using either the conventional method or the post-insertion method [25]. For the conventional method, pre-formed liposomes were incubated with thiolated labeled PAI-2 or TZ (at a molar ratio of 3333:1 liposome phospholipid:protein) for 2 hours at room temperature. For the post-insertion method, micelles composed of 0.8 mM mal-PEG_{2000}-DSPE and 0.2 mM $mPEG_{2000}$-DSPE were prepared as per previously reported methods [26], and labeled PAI-2 or TZ added to the micelles (at a molar ratio of 10:1, mal-PEG_{2000}-DSPE:protein) to form functionalized micelles. Functionalized micelles were added to pre-formed liposomes and heated to 60°C for 1 hour to facilitate post-insertion of micelle lipids into the outer leaflet of the liposomes. Following the liposome functionalization steps, unbound protein was removed from liposomes via repeated centrifugation at 20,000 x g for 1.5 hours at 4°C. Liposomes were resuspended in HEPES buffer (pH 7.4) for single-molecule imaging.

2.4. Intensity measurements for labeled proteins

Microscope coverslips were thoroughly cleaned to remove any hydrophobic and hydrophilic contaminants that could cause background fluorescence from the glass. They were first sonicated for 30 min in ethanol (Chem-Supply, SA, AUS) and then rinsed with deionized water. Subsequently they were sonicated for 30 min in 1 M potassium hydroxide (KOH; Sigma-Aldrich, MO, USA) and rinsed with deionized water again. After these sonication steps were repeated, the coverslips were dried with N_2 [27]. CF labeled proteins were diluted to a concentration of approximately 10 pM and immobilized on the surface of the cleaned microscope coverslip for visualization on an inverted microscope (Nikon Eclipse Ti-E) with a CFI Apo Total Internal Reflection Fluorescence (TIRF) 100x oil-immersion TIRF objective (NA 1.49, Nikon) (Supporting Information Figure S1). The green and red labeled proteins were excited at 1.5 W cm^{-2} with 488 nm (Coherent, Sapphire 488-200 CW) and 647 nm (Coherent, Obis 647-100 CW) lasers, respectively (Supporting Information Figure S1). The signals were separated via dichroic mirrors (Photometrics, DVΛ Multichannel Imaging System) and appropriate filter sets (Chroma). The imaging was done with an EMCCD (Photometics, Evolve 512 Delta). For each measurement, at least two coverslips were used. For each coverslip, multiple (5–10) fields of view were imaged. Using ImageJ (National Institutes of Health, USA) with in-house built plugins, we calculated the integrated intensity for single CF dyes over time, after applying a local background subtraction. Using a change-point step-fitting algorithm, we calculated the intensity distributions for a single CF fluorophore (Figure 1B) [28, 29]. The histograms obtained were fit with a Gaussian distribution function using MATLAB 2014b, to give a mean intensity of 2030 ± 40 for the CF647 (Figure 1C) and 1340 ± 50 for the CF488. To measure the number of fluorophores per protein, we divided the initial fluorescence intensity per protein by the intensity of a single fluorophore (Figure 1D, E).

2.5. Measurement of protein density on liposomes

To find the number of proteins per liposome, we imaged the liposomes under the same conditions and calculated the fluorescence intensity per liposome analogously. We obtained the number of proteins per liposome by dividing these intensities by the intensity of a single protein (Figure 1).

3. Results and Discussion

To visualize proteins attached to liposomes, we labeled 45 kDa human recombinant plasminogen activator inhibitor-2 (PAI-2, SerpinB2) with a small red fluorophore (CF647, 0.8 kDa). The degree of labeling (DOL) was determined by visualizing single proteins using Total Internal Reflection Fluorescence (TIRF) microscopy (Supporting Information Figure S1). Figure 1A shows a typical field of view of individual labeled PAI-2 proteins immobilized on a microscope coverslip. TIRF microscopy allows for the selective excitation of only the fluorescent species on the cover-slip surface and imaging of fluorescence from the surface-immobilized proteins with high contrast and low background. The intensity of the signal of every individual protein can be measured over time (Figure 1B, black line). These intensity trajectories show a stepwise decay towards zero, due to the photobleaching of the fluorophores on the protein. The height of a single step corresponds to the intensity of a single fluorophore. Using an unbiased change-point step-fitting algorithm (Figure 1B, red line) [28], we determined the intensity of a single fluorophore (Figure 1C). By dividing the total intensity per protein by this single-fluorophore intensity we found that there are 1.47 ± 1.21 fluorophores per protein (Figure 1D), with the width of the distribution in line with that expected for a Poisson distribution. These values were confirmed by electrospray ionization mass spectrometry (ESI-MS), which found an average of 3 and up to 6 fluorophores per protein (Supporting Information Figure S2). The same analysis was performed for PAI-2

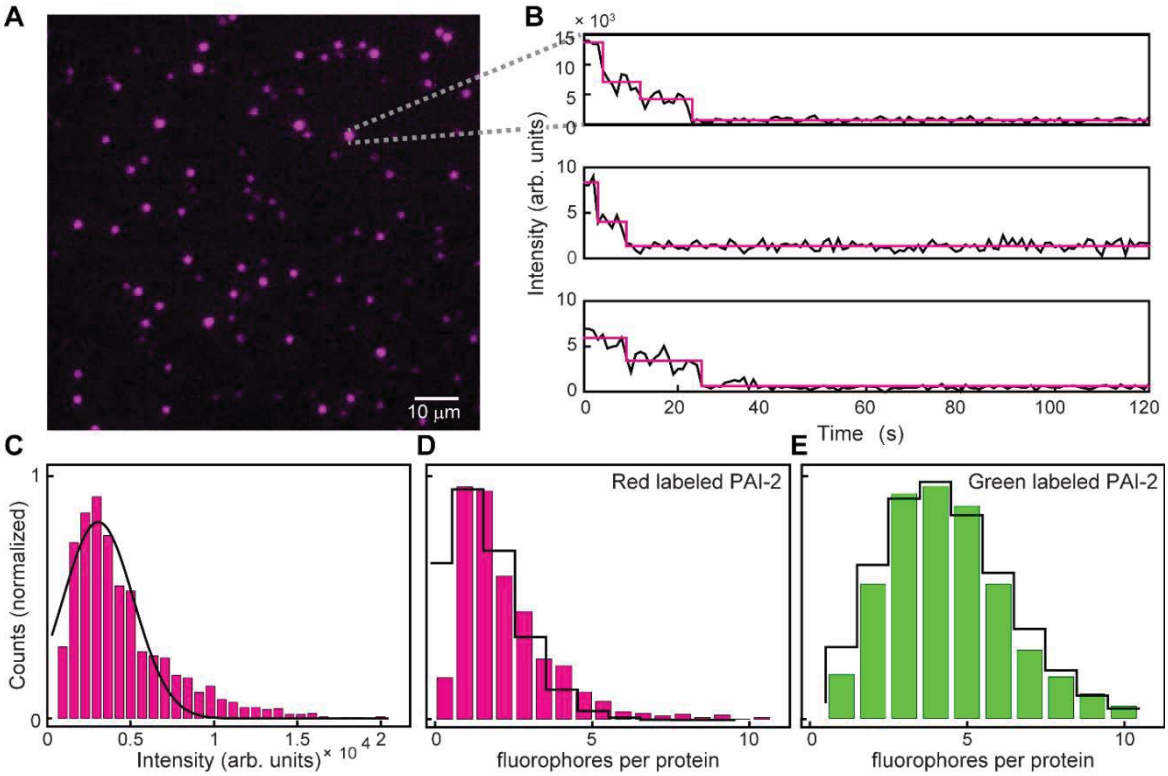

Figure 1. Measurement of the number of fluorophores per protein by TIRF microscopy. (**A**) Typical field of view – red labeled PAI-2 proteins were immobilized on cleaned coverslips. (**B**) Example intensity trajectories of individual labeled proteins (black line). The individual steps were identified using the change-point algorithm (magenta line) [28, 29]. (**C**) Histogram of the intensity of a single CF647 fluorophore, fitted with a Gaussian distribution. The intensity for a single fluorophore is $3 \pm 0.1 \cdot 10^3$ (mean ± s.e.m. $N = 962$). (**D**) Histogram of the number of CF647 fluorophores per protein, fitted with a Poisson distribution. The number of fluorophores is 1.5 ± 0.4 (mean ± s.d. , $N = 291$). (**E**) Histogram of the number of CF488 fluorophores per protein, fitted with a Poisson distribution. This histogram was obtained in the same way as described for CF647 labeled proteins. The intensity for a single fluorophore is $1.2 \pm 0.6 \cdot 10^4$ (mean ± s.e.m., $N = 796$) and the number of fluorophores per protein is 4.5 ± 2.2 (mean ± s.d., $N = 104$).

proteins labeled with a small green fluorophore (CF488, 0.9 kDa) and we obtained an average of 4.5 ± 2.2 fluorophores per protein (Figure 1E). The reproducibility of this method was further confirmed using the same batch of protein measured in independent experiments, where no variation was found between the calculated number. For example, using the PAI-2 protein labeled with CF647 dye, we calculated 1.5 ± 0.4 fluorophores per protein; 4 months later, we repeated the measurement with same protein, and found 2.0 ± 0.6 fluorophores per protein (data not shown).

Liposomes functionalized with red labeled PAI-2 were prepared via the post-insertion method, whereby micelles containing cysteine-reactive poly(ethylene glycol) (maleimide-PEG_{2000}-DSPE) are reacted with protein to form functionalized micelles, before being incubated with pre-formed liposomes to promote insertion of the protein-PEG_{2000}-DSPE conjugate into the outer leaflet of the liposome [30]. Liposomes were visualized using TIRF microscopy under the same conditions that were used to determine the number of fluorophores per protein. To confirm that the fluorescence signal observed in these experiments originates from proteins bound to single liposomes, we prepared the liposomes in the presence of the fluorophore R18 (Octadecyl Rhodamine B Chloride) so that the encapsulated R18 acts as a marker for only those liposomes that have an intact lipid bilayer [31]. Using optics that split the image in a yellow and a red channel, the R18 labeled liposomes and the red labeled proteins were visualized simultaneously but each on different areas of the camera sensor. Figure 2A represents a typical field of view showing the R18 fluorescence (left), the signal from the red labeled proteins (middle), and a merge of the two signals (right), with colocalization indicated by white spots. Based on these images, we calculated that 88% of liposomes have at least one protein attached. Liposomes prepared with on-maleimide-functionalized micelles were used to confirm that only covalently attached proteins colocalize with liposomes in imaging experiments (Supporting Information Figure

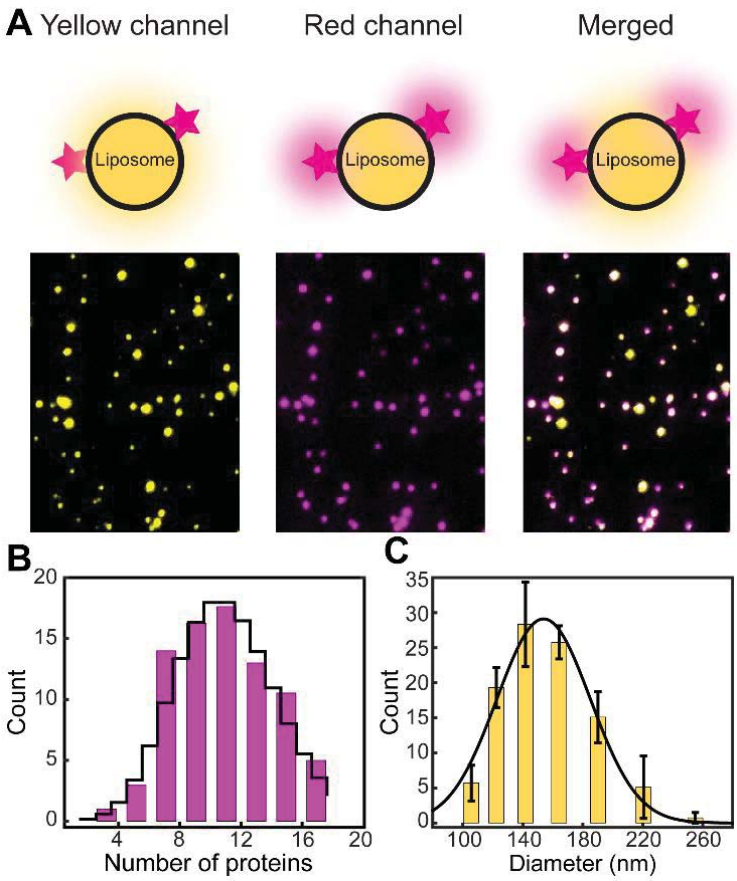

Figure 2. Visualization of proteins attached to liposomes. (**A**) Liposomes labeled with R18 (left) and proteins (middle) were imaged simultaneously (N = 14 fields of view, ~30 liposomes per field of view). A merge of the two channels (right) showed a high degree of colocalization (white spots). (**B**) Histogram of the number of proteins per liposome, fitted with a Poisson distribution (black line). The number of proteins is 11 ± 4 (mean ± s.d.) (**C**) Histogram of the diameter of the liposomes measured by dynamic light scattering, fitted with a Gaussian distribution (black line). The diameter is 153 ± 56. Bars represent the mean ± s.d. (n = 3).

S3). We then determined the number of proteins per liposome using the fluorescence intensity from the labeled proteins. We divided this intensity by the intensity of a single protein, obtained earlier (Figure 1D). We found a density of 11 ± 4 (mean ± s.d.) proteins per liposome (Figure 2B). Dynamic light scattering revealed a liposome diameter of 153 ± 56 nm

(mean ± s.d.) and a polydispersity index of 0.041 ± 0.017 (mean ± s.d.) (Figure 2C). If we calculate the relative width of the distributions in Figures 2B and 2C, we find that this is 0.36 for both distributions. Therefore, we conclude that the width of the distribution of the number of proteins per liposome correlates with the intrinsic width of the liposome size distribution. Larger liposomes thus have a greater number of proteins attached than smaller liposomes.

To explore the ability of single-molecule imaging to quantify differences in protein density, we varied the stoichiometry of two differently labeled proteins and quantified their ratio on the liposome surface. To negate any potential effects that would arise from using two different proteins, such as size and reactivity, we used only PAI-2 proteins. Dual-ligand liposomes were prepared via the post-insertion method, using red and green labeled PAI-2 at molar ratios of 1:1, 2:1, 5:1 and 10:1, while keeping the total amount of protein added constant. The two proteins were visualized simultaneously using dual-color imaging (Figure 3A) and the protein density was determined as above. At a 1:1 molar ratio, we found 51 ± 2 % of the total number of proteins per liposome had a red label and 49 ± 2 % had a green label (Figure 3B). This observation indicates that the fluorophores do not affect protein attachment, and that the two proteins are incorporated in the same 1:1 ratio as their input stoichiometry in the formulation process. Further analysis revealed that changing the ratios of the two labeled proteins during preparation similarly altered the ratios of proteins incorporated into the liposome (Figure 3C, Supporting Information Figure S4). These results highlight the accuracy of the single-molecule measurements, and illustrate the ability of this method to report on small differences in protein densities and ratios.

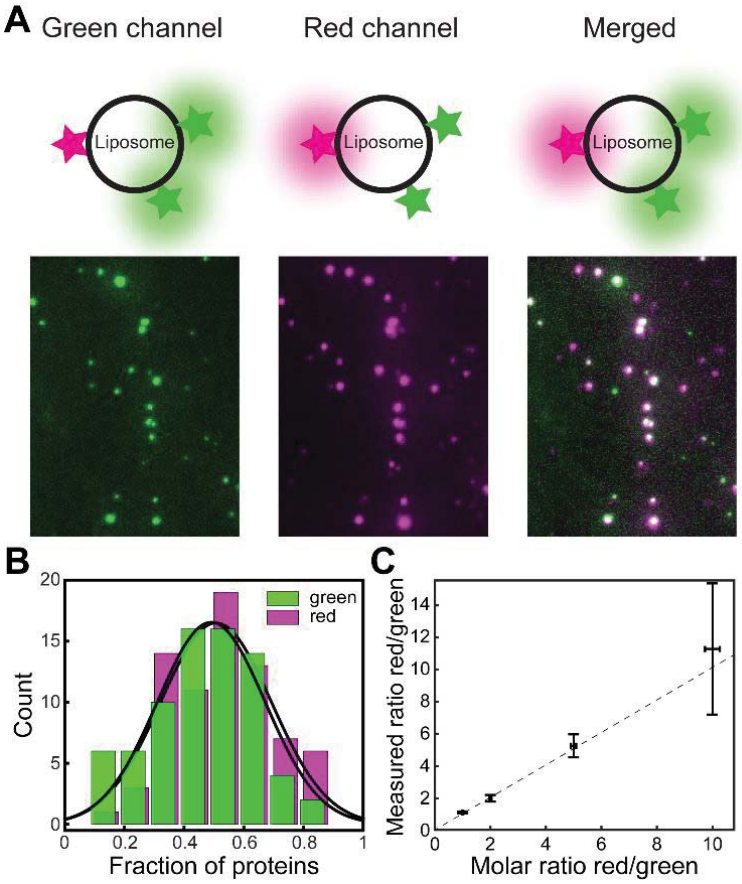

Figure 3. Quantification of the number of proteins per liposome. (**A**) Typical field of view showing dual-ligand immobilized liposomes. The green (left) and red dyes (middle) were visualized simultaneously. When the two channels are merged, colocalized spots show up as white (right). (**B**) Histograms of the measured fraction of green and red labeled proteins per liposome, when equal amounts of each were used during preparation. The fraction of green labeled proteins is 0.49 ± 0.02 and the fraction of red proteins is 0.51 ± 0.02. (**C**) Measured ratio of the fraction of red labeled proteins over the fraction of green labeled proteins as a function of the molar ratio used during preparation. The errors in the molar ratio are pipetting errors calculated from the manufacturer-published imprecision ranges of the pipettes used to add the micelle volumes to the liposomes during preparation. The errors in the measured ratio are the s.e.m.

Finally, we demonstrated the utility of single-molecule quantification in the characterization of novel clinically-relevant ligand-directed liposomes. Dual-ligand liposomes were prepared via both the conventional and the post-insertion methods of liposome functionalization (Figure 4A). The conventional method involves the incorporation of polyethylene glycol (PEG) chains with a terminal maleimide functional group (maleimide-PEG-DSPE) into the lipid bilayer of the liposome during formation. Pre-formed liposomes are then incubated with two different thiolated proteins at 25°C, which attach covalently to the liposome surface via the maleimide moiety. The post-insertion method involves the creation of maleimide-PEG-DSPE micelles to which proteins are covalently attached as per the conventional method. Micelles are then incubated with pre-formed liposomes at a temperature of 60°C to facilitate the transfer of the micelle PEG-DSPE and attached ligands into the outer leaflet of the liposome bilayer. In this experiment, PAI-2 and trastuzumab (TZ, Herceptin®, 145 kDa) were labeled with red and green dyes, respectively, and added to pre-formed liposomes in a 1:1 molar ratio. Imaging and data analysis were performed as outlined above. Using our single-molecule imaging approach, we determined that the ratio of the PAI-2 and TZ incorporated into liposomes was closer to 1 for liposomes prepared via the post-insertion method (ratio = 2.1 ± 2.5) than for liposomes prepared via the conventional method (ratio = 17 ± 18) (Figure 4B).

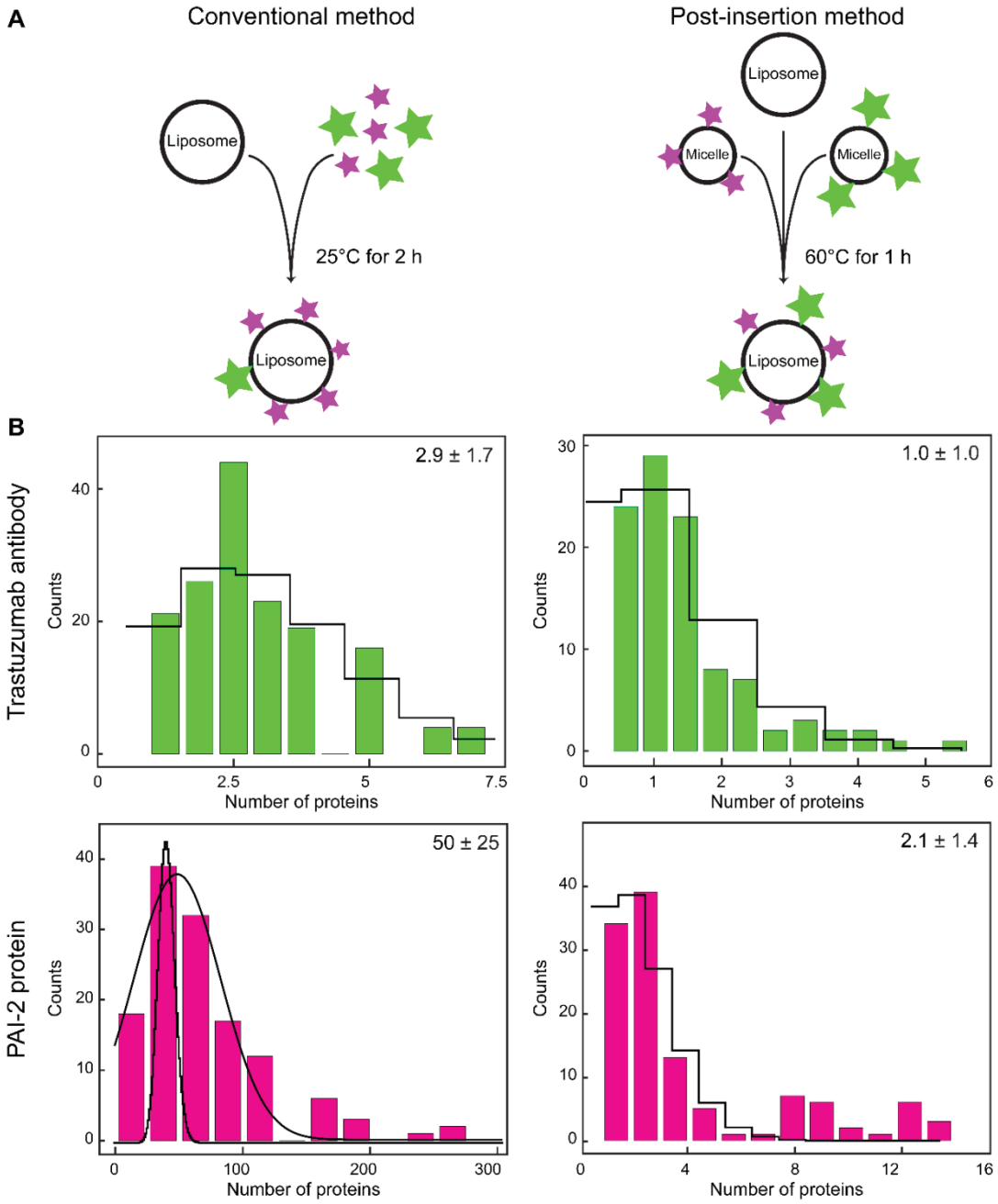

Figure 4. Conventional and post-insertion methods for dual-ligand liposome preparation. (**A**) In the conventional method, pre-formed liposomes are incubated with two different thiolated proteins (represented by green and magenta stars), which attach covalently to the liposome surface via the maleimide moiety. The post-insertion method involves the creation of protein-conjugated micelles, which are then incubated with pre-formed liposomes at a temperature of 60°C to facilitate the transfer of the micelle phospholipids and attached ligands into the outer leaflet of the liposome bilayer. (**B**) Comparison of the number of proteins per liposome

prepared via the conventional and post-insertion methods. When using a 1:1 ratio of trastuzumab antibody to PAI-2 protein in the conventional preparation method, the number of PAI-2 proteins per liposome was ~17 times higher than the number of trastuzumab antibodies (top, $N = 115$). These numbers were much more similar when the post-insertion method was used (bottom, $N = 167$). The black lines represent Poisson distribution fits to the histograms. Due to the large number of proteins in the top right panel, heterogeneities within the sample broaden the histogram and obscure the Poisson distribution. This histogram was therefore fitted with a Gaussian distribution.

The conventional method involves incubation of a small protein and a large antibody with pre-formed liposomes, where differences in protein size (i.e. steric hindrance on rates of reaction) and reactivity (i.e. number of available sites for conjugation) may affect their equal incorporation into the liposomes. In contrast, the post-insertion method helps negate effects of these protein differences through the simultaneous insertion of two separate pre-formed protein-functionalized micelles into the liposomes [25]. These results provide a rationale for use of the post-insertion method in the production of dual-ligand liposomes functionalized with two very different proteins in terms of their size and/or reactivity. The application of the single-molecule quantification informing on the preparation protocol allows for a better control of the stoichiometry of the liposomes produced.

4. Conclusion

Herein, we have demonstrated the practical utility of single-molecule fluorescence imaging in the quantification of the density of protein ligands attached to the surface of liposomes. This method enables the quantitative characterization of protein densities and the ability to detect changes therein. While the work presented here explored the quantification of protein and

whole antibody ligands on the surface of liposomes, the single-molecule approach is also suitable for quantifying other liposome ligand types, such as antibody fragments, small peptides and aptamers, provided that they can be fluorescently labeled for single-molecule imaging. Furthermore, the method permits future experiments to elucidate additional characteristics of ligand-directed liposomes, including the quantification of inner leaflet and outer leaflet labeling of liposomes using environmentally (e.g. pH) sensitive dyes [32]. The use of single-molecule imaging as a quantification technique could improve the characterization of preclinical ligand-directed liposomes, assist with large-scale manufacturing processes and allow for batch-to-batch quality control in a commercial production setting. Using this technique, we showed that the post-insertion method of ligand-coupled liposome preparation is the preferred method for dual-ligand liposomes when using proteins of different sizes – an aspect relevant to the clinical setting, where liposomes used to target heterogeneous tumor cell populations would likely bear two different targeting ligands. By enabling the quantification of surface-bound ligands, and informing on optimal preparation protocols for ligand-directed liposomes, this single-molecule quantitative approach is expected to improve the preclinical development of targeted liposomal drug delivery systems intended for clinic use.

Acknowledgements

This research has been conducted with the support of a Cure Cancer Australia Foundation (CCAF) Project Grant, the Centre for Medical and Molecular Bioscience (University of Wollongong; UOW), an Australian Government Research Training Program Scholarship, and a Jayne Wilson Cancer Research PhD Top-Up Scholarship (UOW). CCAF: Kara L. Vine APP1045831; Australian Research Council (ARC): Antoine M. van Oijen, DP150100956; Australian Research Council (ARC): Antoine M. van Oijen, FL140100027; Fundamenteel

onderzoek der materie (FOM): Lisanne M. Spenkelink, 12CMCE03. We thank Celine Kelso for assistance with the ESI-MS analysis.

Competing interests

The authors have no competing interests to declare.

References

1. Grimaldi, N., et al., *Lipid-based nanovesicles for nanomedicine.* Chemical Society Reviews, 2016. **45**(23): p. 6520-6545.
2. Allen, T.M. and P.R. Cullis, *Liposomal drug delivery systems: From concept to clinical applications.* Adv. Drug Delivery Rev., 2013. **65**(1): p. 36-48.
3. Nichols, J.W. and Y.H. Bae, *EPR: Evidence and fallacy.* Journal of Controlled Release, 2014. **190**: p. 451-64.
4. Gerlowski, L.E. and R.K. Jain, *Microvascular permeability of normal and neoplastic tissues.* Microvasc Res, 1986. **31**(3): p. 288-305.
5. Barenholz, Y., *Doxil(R)--the first FDA-approved nano-drug: lessons learned.* J Control Release, 2012. **160**(2): p. 117-34.
6. Ishida, T., D.L. Iden, and T.M. Allen, *A combinatorial approach to producing sterically stabilized (Stealth) immunoliposomal drugs.* FEBS Letters, 1999. **460**(1): p. 129-133.
7. Pattni, B.S., V.V. Chupin, and V.P. Torchilin, *New Developments in Liposomal Drug Delivery.* Chemical Reviews, 2015. **115**(19): p. 10938-66.
8. Wilhelm, S., et al., *Analysis of nanoparticle delivery to tumours.* Nat. Rev. Mater., 2016. **1**: p. 16014.

9. Laginha, K., D. Mumbengegwi, and T. Allen, *Liposomes targeted via two different antibodies: Assay, B-cell binding and cytotoxicity.* BBA - Biomembranes, 2005. **1711**: p. 25-32.
10. Doolittle, E., et al., *Spatiotemporal Targeting of a Dual-Ligand Nanoparticle to Cancer Metastasis.* ACS Nano, 2015. **9**(8): p. 8012-21.
11. Estanqueiro, M., et al., *Evolution of liposomal carriers intended to anticancer drug delivery: an overview.* Int. J. Curr. Pharm. Res., 2014. **6**(4): p. 8.
12. Shi, J., et al., *Cancer nanomedicine: progress, challenges and opportunities.* Nat Rev Cancer, 2017. **17**(1): p. 20-37.
13. Lukyanov, A.N., et al., *Tumor-targeted liposomes: doxorubicin-loaded long-circulating liposomes modified with anti-cancer antibody.* Journal of Controlled Release, 2004. **100**(1): p. 135-144.
14. Park, J.W., et al., *Tumor targeting using anti-her2 immunoliposomes.* Journal of Controlled Release, 2001. **74**: p. 95-113.
15. Anchordoquy, T.J., et al., *Mechanisms and Barriers in Cancer Nanomedicine: Addressing Challenges, Looking for Solutions.* ACS Nano, 2017. **11**(1): p. 12-18.
16. Hare, J.I., et al., *Challenges and strategies in anti-cancer nanomedicine development: An industry perspective.* Advanced Drug Delivery Reviews, 2017. **108**: p. 25-38.
17. Caracciolo, G., O.C. Farokhzad, and M. Mahmoudi, *Review: Biological Identity of Nanoparticles In Vivo: Clinical Implications of the Protein Corona.* Trends in Biotechnology, 2017. **35**: p. 257-264.
18. Klegerman, M.E., et al., *Quantitative Immunoblot Assay for Assessment of Liposomal Antibody Conjugation Efficiency.* Analytical Biochemistry, 2002. **300**(1): p. 46.
19. Mack, K., et al., *Dual Targeting of Tumor Cells with Bispecific Single-Chain Fv-Immunoliposomes.* Antibodies, 2012. **1**(2): p. 199-214.

20. Monachino, E., L.M. Spenkelink, and A.M. van Oijen, *Watching cellular machinery in action, one molecule at a time.* J Cell Biol, 2017. **216**(1): p. 41-51.
21. Marchetti, M., et al., *How to switch the motor on: RNA polymerase initiation steps at the single-molecule level.* Protein Sci, 2017.
22. Aggarwal, V. and T. Ha, *Single-molecule fluorescence microscopy of native macromolecular complexes.* Curr Opin Struct Biol, 2016. **41**: p. 225-232.
23. Cochran, B.J., et al., *The CD-loop of PAI-2 (SERPINB2) is redundant in the targeting, inhibition and clearance of cell surface uPA activity.* BMC Biotechnol, 2009. **9**: p. 43.
24. Uster, P.S., et al., *Insertion of poly(ethylene glycol) derivatized phospholipid into pre-formed liposomes results in prolonged in vivo circulation time.* FEBS Lett, 1996. **386**(2-3): p. 243-6.
25. Iden, D.L. and T.M. Allen, *In vitro and in vivo comparison of immunoliposomes made by conventional coupling techniques with those made by a new post-insertion approach.* BBA - Biomembranes, 2001. **1513**(2): p. 207-216.
26. Moreira, J.N., et al., *Use of the post-insertion technique to insert peptide ligands into pre-formed stealth liposomes with retention of binding activity and cytotoxicity.* Pharmaceutical Research, 2002. **19**(3): p. 265-269.
27. Tanner, N.A. and A.M. van Oijen, *Visualizing DNA replication at the single-molecule level.* Methods Enzymol, 2010. **475**: p. 259-78.
28. Duderstadt, K.E., et al., *Simultaneous Real-Time Imaging of Leading and Lagging Strand Synthesis Reveals the Coordination Dynamics of Single Replisomes.* Mol Cell, 2016. **64**(6): p. 1035-1047.
29. Watkins, L.P. and H. Yang, *Detection of intensity change points in time-resolved single-molecule measurements.* J Phys Chem B, 2005. **109**(1): p. 617-28.

30. Allen, T.M., P. Sapra, and E. Moase, *Use of the post-insertion method for the formation of ligand-coupled liposomes.* Cellular & Molecular Biology Letters, 2002. **7**(3): p. 889-894.

31. Serro, A.P., et al., *Formation of an intact liposome layer adsorbed on oxidized gold confirmed by three complementary techniques: QCM-D, AFM and confocal fluorescence microscopy.* Surf. Interface Anal., 2012. **44**(4): p. 426-433.

32. Otterstrom, J.J., et al., *Relating influenza virus membrane fusion kinetics to stoichiometry of neutralizing antibodies at the single-particle level.* Proc Natl Acad Sci U S A, 2014. **111**(48): p. E5143-8.

Graphical abstract

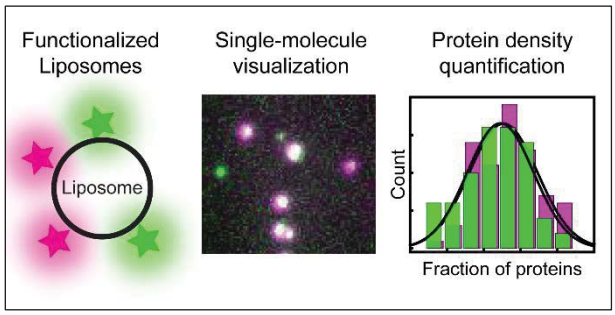

Figure(s)
Click here to download high resolution image

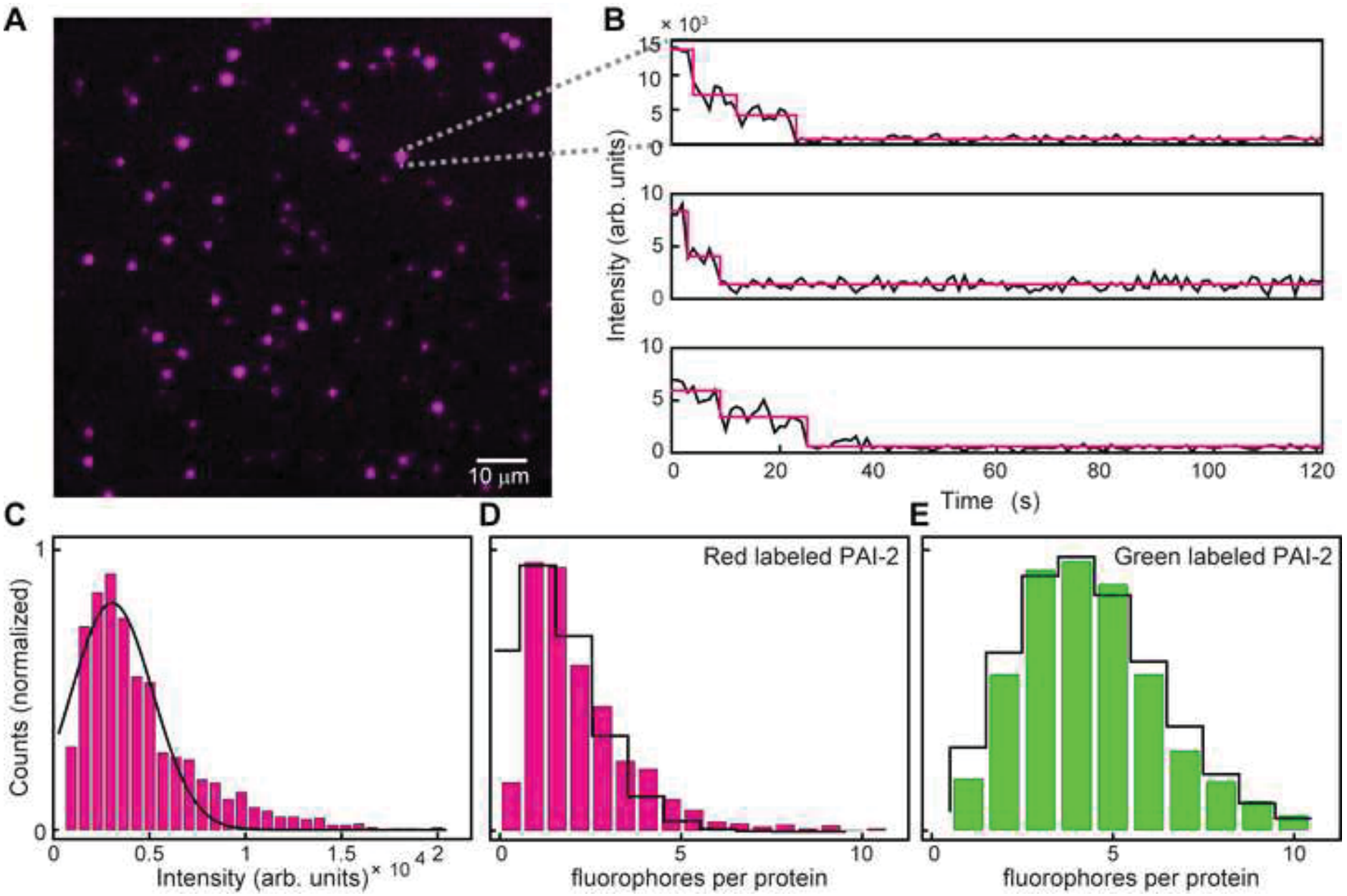

Figure(s)
Click here to download high resolution image

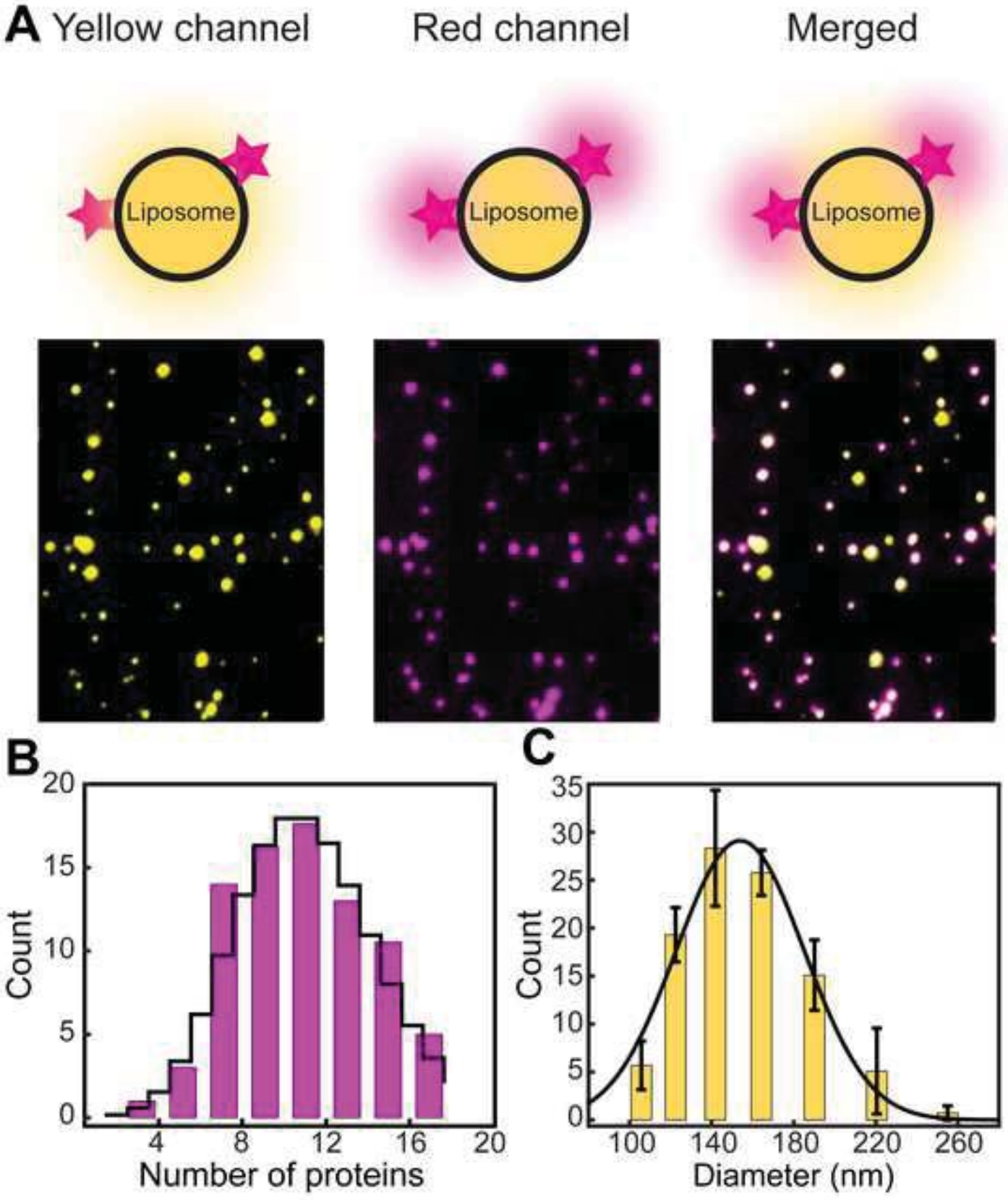

Figure(s)
Click here to download high resolution image

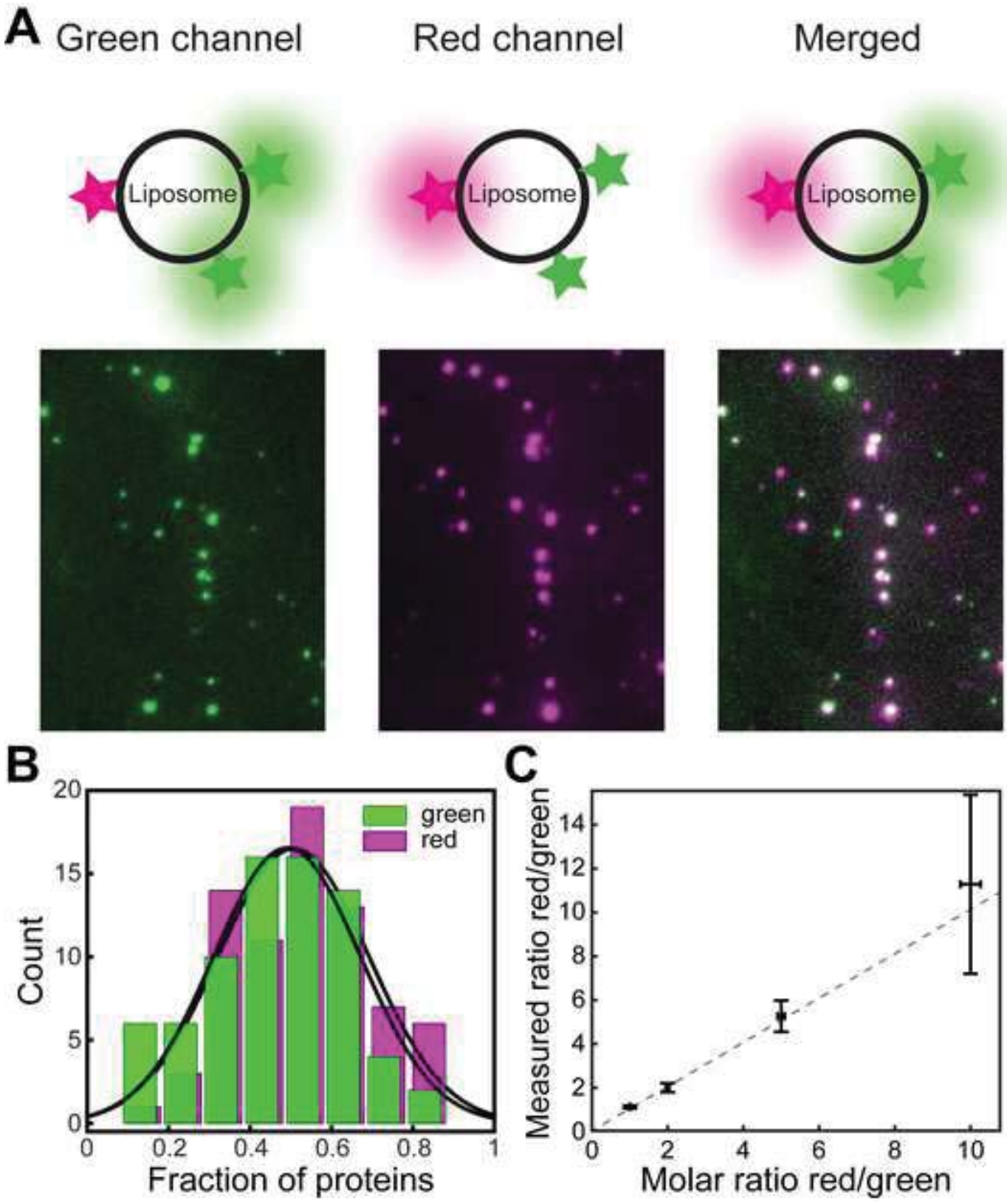

Figure(s)
Click here to download high resolution image

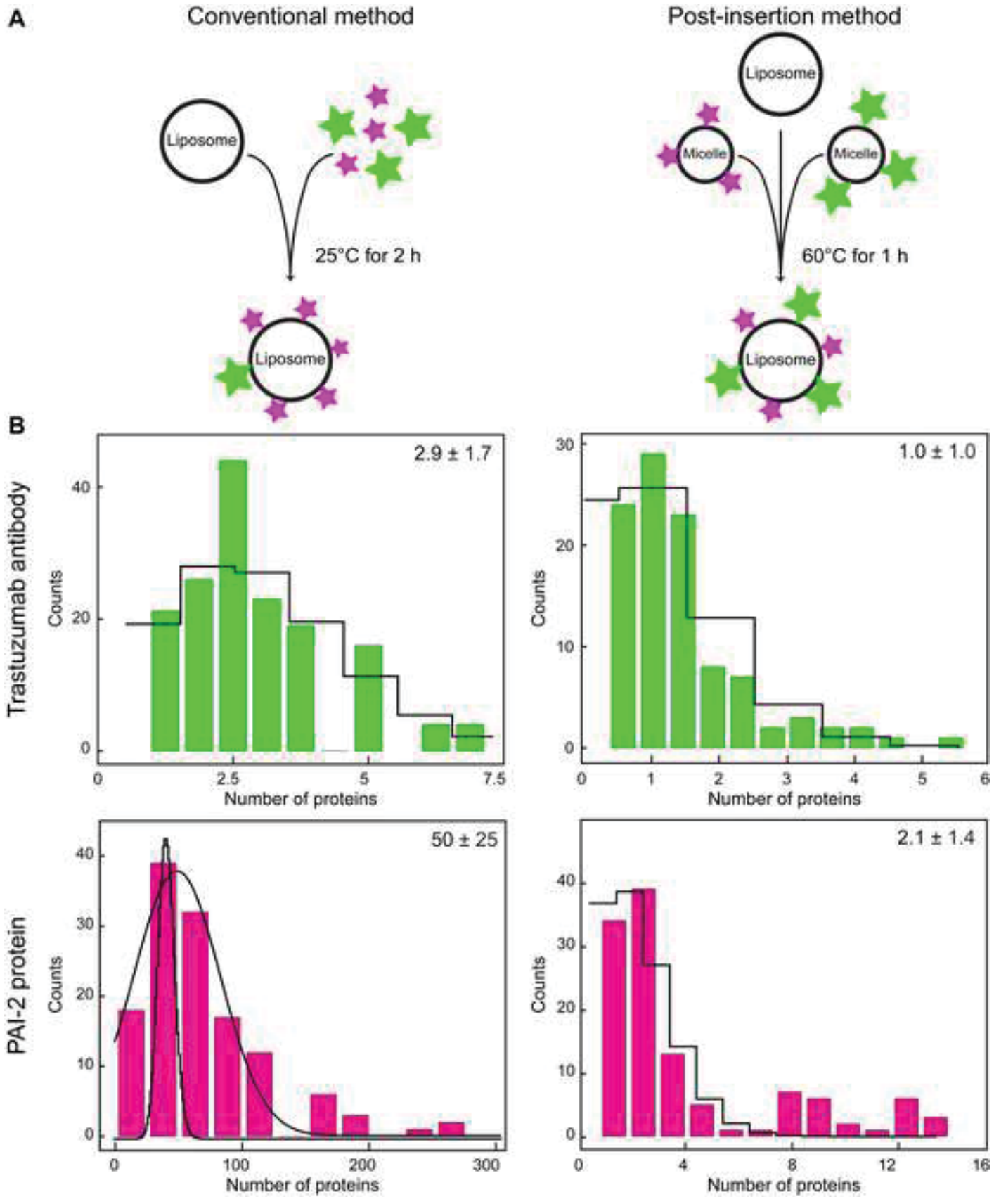

Revised Supplementary Material

Click here to download Supplementary Material: JCRSuppContentForResubmission_FINAL.docx